

Undular Tidal Bores: Basic Theory and Free-Surface Characteristics

Hubert Chanson¹

Abstract: The present study examines the free-surface properties of undular tidal bores observed for $1 < F < 1.5$ – 1.8 . The analysis is based on some new experimental results together with a reanalysis of both field and laboratory data. The free-surface profiles followed a pattern somehow similar to the sinusoidal and cnoidal wave shapes, although neither captures the fine details of the undulation profiles. The wave properties highlighted some maxima in amplitude and steepness for a Froude number of about 1.3 – 1.4 corresponding to the apparition of some wave breaking at the first wave crest.

DOI: 10.1061/(ASCE)HY.1943-7900.0000264

CE Database subject headings: Free surfaces; Wave crest; Tidal currents; Laboratory tests; Data analysis.

Author keywords: Undular tidal bores; Free-surface undulations; Surface profile; Laboratory data; Field data.

Introduction

A tidal bore is a series of waves propagating upstream as the tidal flow turns to rising. It forms during spring tides with macrotidal conditions when the flood tide is confined to a narrow funneled estuary that amplifies the tidal wave (Peregrine 1966). When the Froude number is larger than and close to unity, the bore front is followed by a train of secondary waves called undulations or whelps (Lemoine 1948; Benjamin and Lighthill 1954). An undular bore may also be observed in irrigation channels and water power canals during gate operation (Benet and Cunge 1971; Treske 1994).

The present study examines the free-surface properties of undular tidal bores. The analysis is based on some new experimental results together with a reanalysis of both field and laboratory data. It is the aim of this work to characterize some seminal features of undular tidal bores.

Experimental Facility and Instrumentation

The new experiments were performed in a 0.5 -m-wide, 12 -m-long rectangular horizontal channel. The flume was made of smooth PVC bed and glass walls. A radial gate was located at the channel downstream end ($x = 11.9$ m) to create a range of initially steady subcritical flow conditions. A fast-closing tainter gate was located next to and just upstream of the radial gate at $x = 11.15$ m (Fig. 1).

The water discharge was measured with orifice meters with an accuracy of less than 2% . In steady flows, the water depths were measured using rail mounted pointer gauges. The unsteady water

depths were measured with a series of acoustic displacement meters Microsonic Mic+25/IU/TC spaced along the channel at $x = 8.0, 6.0, 5.0, 4.55, 4.0,$ and 3.0 m, where x = longitudinal distance from the channel upstream end. The experiments were conducted for a range of flow conditions summarized in Table 1. The downstream radial gate located at $x = 11.9$ m controlled the initial steady flow depth d_o and velocity V_o (Fig. 1), and its opening was kept constant during each experiment. The steady flow conditions were established for at least 15 min prior to each series of measurements. Further details were reported in Chanson (2009).

The tidal bore was generated by the rapid (partial or complete) closure of the tainter gate. Its closure time was less than 0.2 s. After closure, the bore propagated upstream, and each experiment was stopped when the bore reached the intake structure. The bore properties were recorded at $x = 5$ m, where the steady flow was partially developed. The relative boundary layer thickness was about $\delta/d_o = 0.3$ – 0.4 depending on the flow conditions.

Basic Flow Patterns

The visual observations and free-surface measurements highlighted several flow patterns depending on the tidal bore Froude number defined as

$$F = \frac{V_o + U}{\sqrt{g \times d_o}} \quad (1)$$

where U = surge front celerity positive upstream and g = gravity acceleration. F is the Froude number defined in the system of coordinates in translation with the bore (Henderson 1966; Liggett 1994).

For $F < 1.5$ – 1.6 , the tidal bore was followed a train of well-formed undulations: i.e., an undular tidal bore. The undular bore had a smooth, quasi-two-dimensional profile for $F < 1.25$. For $1.25 < F$, some slight cross waves (shock waves) were observed, starting next to the sidewalls upstream of the first wave crest and intersecting next to the first crest. A similar cross-wave pattern was observed in stationary undular hydraulic jumps and in undular tidal bores (Chanson and Montes 1995; Koch and Chanson

¹Professor, School of Civil Engineering, The Univ. of Queensland, Brisbane, Queensland 4072, Australia. E-mail: h.chanson@uq.edu.au

Note. This manuscript was submitted on August 11, 2009; approved on April 23, 2010; published online on April 27, 2010. Discussion period open until April 1, 2011; separate discussions must be submitted for individual papers. This technical note is part of the *Journal of Hydraulic Engineering*, Vol. 136, No. 11, November 1, 2010. ©ASCE, ISSN 0733-9429/2010/11-940-944/\$25.00.

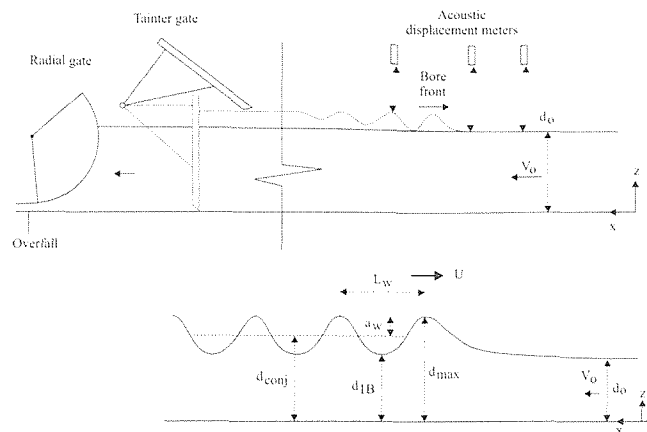


Fig. 1. Sketch of the experimental facility and details of the undular bore front

2008). For $1.3 < F < 1.5-1.6$, some slight wave breaking was further observed at the first wave crest, and the free-surface undulations became flatter. The cross waves were also observed. For the largest bore Froude numbers (i.e., $F > 1.5-1.6$), the tidal bore was characterized by a marked roller. The free surface appeared to be quasi-two-dimensional behind the breaking bore, and some air entrainment was observed in the roller.

For the entire range of investigations, the basic flow patterns were consistent with the earlier findings of Favre (1935) and others (Table 1). Noteworthy, the flow patterns were basically inde-

pendent of the initial steady flow Froude number $Fr_o = V_o / \sqrt{g \times d_o}$.

Free-Surface Properties of Undular Tidal Bores

A key feature of undular bores is the secondary wave motion illustrated in Fig. 2 with the dimensionless time variations in the water depth at several longitudinal distances for two Froude numbers ($F=1.11$ and 1.22). In tidal bores and hydraulic jumps, the equation of conservation of momentum may be applied across the jump front together with the equation of conservation of mass (Henderson 1966; Liggett 1994; Chanson 1999). When the rate of energy dissipation is negligible as in an undular tidal bore, there is a quasi-conservation of energy. Let us follow the tidal bore in the system of coordinates in translation with the undular bore front. The equations of conservation of momentum and energy may be rewritten as

$$\frac{M}{d_c^2} = \frac{d_c}{d} + \frac{1}{2} \times \left(\frac{d}{d_c} \right)^2 = \text{const} \quad (2)$$

$$\frac{E}{d_c} = \frac{d}{d_c} + \frac{1}{2} \times \left(\frac{d_c}{d} \right)^2 = \text{const} \quad (3)$$

where M =momentum function; E is similar to the energy per unit mass, also called the specific energy; and d =flow depth. For a tidal bore, d_c equals

Table 1. Experimental Investigations of Tidal Bores and Positive Surges

Reference	Initial flow		Bore direction	Channel geometry	Remarks
	V_o (m/s)	d_o (m)			
(a) Laboratory experiments					
Favre (1935)	0	0.106–0.206	U/S	Rectangular ($B=0.42$ m) $\theta=0^\circ$	Flume length: 73.8 m
	$\neq 0$	0.109–0.265	U/S	Rectangular ($B=0.42$ m) $\theta=0.017^\circ$	
Benet and Cunge (1971)	0–0.198	0.057–0.138	D/S	Trapezoidal (base width: 0.172 m, sideslope: 2H:1V) $\theta=0.021^\circ$	Flume length: 32.5 m
Treske (1994)		0.08–0.16	U/S	Rectangular ($B=1$ m) $\theta=0.001^\circ$	Flume length: 100 m, concrete channel
		0.04–0.16	U/S,D/S	Trapezoidal (base width: 1.24 m, sideslope: 3H:1V) $\theta=0^\circ$	Flume length: 124 m, concrete channel
Koch and Chanson (2008, 2009)	1.0	0.079	U/S	Rectangular ($B=0.50$ m) $\theta=0^\circ$, PVC invert	Flume length: 12 m
Chanson (2010)	0.83	0.137	U/S	Rectangular ($B=0.50$ m) $\theta=0^\circ$, PVC invert	Flume length: 12 m
	0.83	0.142	U/S	Rectangular ($B=0.50$ m) $\theta=0^\circ$, rough screen invert	
Present study	0.19–0.92	0.056–0.20	U/S	Rectangular ($B=0.50$ m) $\theta=0^\circ$, PVC invert	Flume length: 12 m
(b) Field experiments					
Benet and Cunge (1971)	0.59–1.08	6.61–9.16	U/S	Trapezoidal (base width: 9 m, sideslope: 2H:1V) $\theta=0.006-0.0086^\circ$	Oraison power plant intake channel
	1.51–2.31	5.62–7.53	U/S	Trapezoidal (base width: 8.6 m, sideslope: 2H:1V)	Jouques-Saint Estève intake channel
Lewis (1972)	0–0.2	0.9–1.4	U/S	Dee River near Saltney Ferry footbridge; trapezoidal channel	Field experiments between March and September 1972
Navarre (1995)	0.65–0.7	1.12–1.15	U/S	Dordogne River at Port de Saint Pardon; width ~ 290 m	Field experiments on April 25 and 26, 1990
Wolanski et al. (2004)	0.15	1.5–4	U/S	Daly River. Width ~ 140 m	Field experiments in July and September 2002 and on July 2, 2003

Note: B =channel width; d_o =initial water depth; V_o =initial flow velocity; θ =bed slope angle with the horizontal; bore direction, U/S=propagating upstream; D/S=propagating downstream; and (—)=information not available.

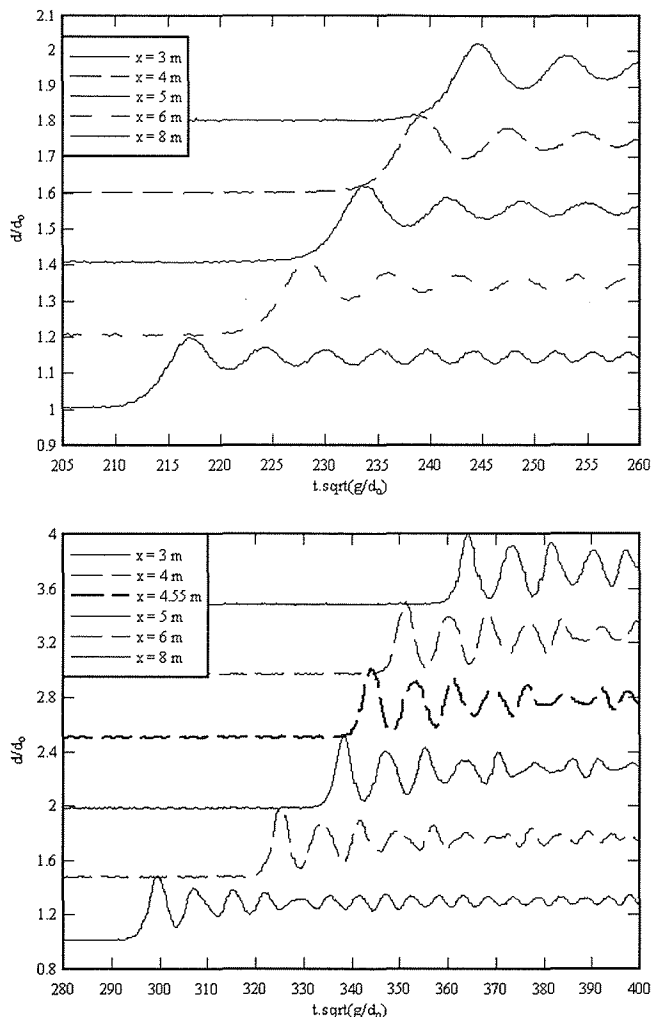


Fig. 2. Dimensionless time variations in the flow depth during the propagation of an undular tidal bore; each curve was offset vertically by 0.2: (a) $Q=0.0190 \text{ m}^3/\text{s}$, $d_o=0.191 \text{ m}$, $F=1.11$, $U=1.32 \text{ m/s}$, and Run 090417_64; (b) $Q=0.0089 \text{ m}^3/\text{s}$, $d_o=0.0802 \text{ m}$, $F=1.22$, $U=0.862 \text{ m/s}$, and Run 090417_62

$$d_c = \sqrt[3]{\frac{[(V_o + U) \times d_o]^2}{g}} \quad (4)$$

Eq. (2) is always valid but Eq. (3) is an approximation only applicable to an undular tidal bore with a small Froude number close to unity. In which case, Eqs. (2) and (3) may be considered as a parametric representation of the relationship between the dimensionless momentum M/d_c^2 and energy E/d_c (Benjamin and Lighthill 1954; Montes 1986). The function $M-E$ has two branches intersecting at $M/d_c^2=1.5$ and $E/d_c=1.5$ [Fig. 3(a)]. The two branches represent the only possible relationship between M/d_c^2 and E/d_c in a tidal bore as long as both Eqs. (2) and (3) hold. The right branch of the curve $M-E$ corresponds to the supercritical flow while the upper branch (or left branch) corresponds to a subcritical flow. Fig. 3(b) presents a comparison between Eqs. (2) and (3) and some data. The graph includes the initial flow conditions (symbol *) and the undular flow data between the first and fourth wave crests. The data justified the approximation of negligible energy losses [Eq. (3)]: all the data were located on the parametric curve $M-E$. Further the quasi-totality of the undular flow data was on the subcritical

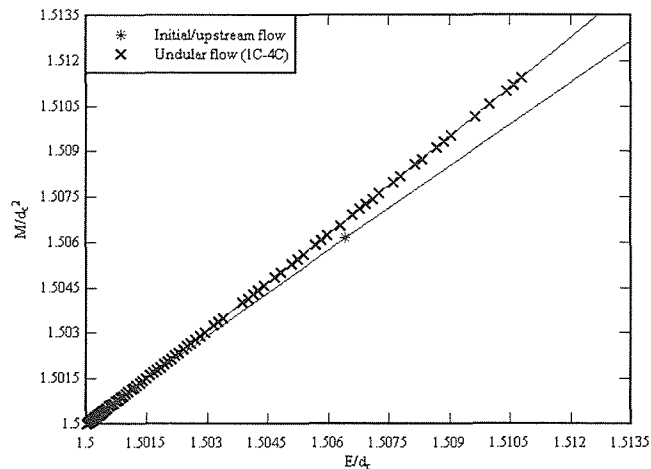
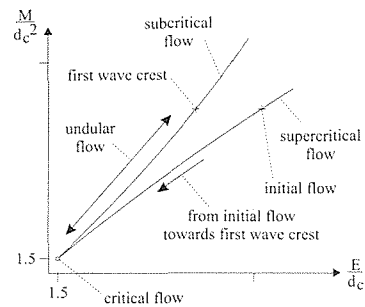


Fig. 3. Dimensionless relationship between the momentum and energy fluxes in undular tidal bores: (a) definition sketch; (b) experimental data: $Q=0.0299 \text{ m}^3/\text{s}$, $d_o=0.2055 \text{ m}$, $F=1.10$, $U=1.316 \text{ m/s}$, $x=5 \text{ m}$, and Run 090304_15

flow branch of the $M-E$ curve. Note a seemingly greater momentum and specific energy at the first wave crest than in the initial flow. This was because Eqs. (2) and (3) are based on the assumption of hydrostatic pressure distribution; but the free-surface curvature at the wave crest implies a pressure gradient less than hydrostatic, hence a smaller specific energy, for example.

Undular Profile

The secondary wave motion presents a smooth undular shape (Figs. 2 and 4). Fig. 4 shows both field and laboratory data, and the data are compared with the linear wave theory (sinusoidal curve) and Boussinesq equation solution (cnoidal wave function) (Lemoine 1948; Benjamin and Lighthill 1954). Both functions were fitted between a crest/trough and the adjacent trough/crest over each half-wavelength. Altogether there was a poor agreement between the data and mathematical functions: neither the linear wave theory nor the Boussinesq equations captured the fine details of the free-surface profile shape nor the asymmetrical wave shape. Noteworthy, the comparison showed the largest deviations between sinusoidal and cnoidal wave functions between a wave crest and trough, and some lesser differences between a wave trough and subsequent crest (Fig. 4). The experimental observations highlighted the asymmetry of the free-surface undulations. The undulation asymmetry was already noted in the stationary undular hydraulic jumps in terms of both the free-surface profile and the vertical distributions of pressure and ve-

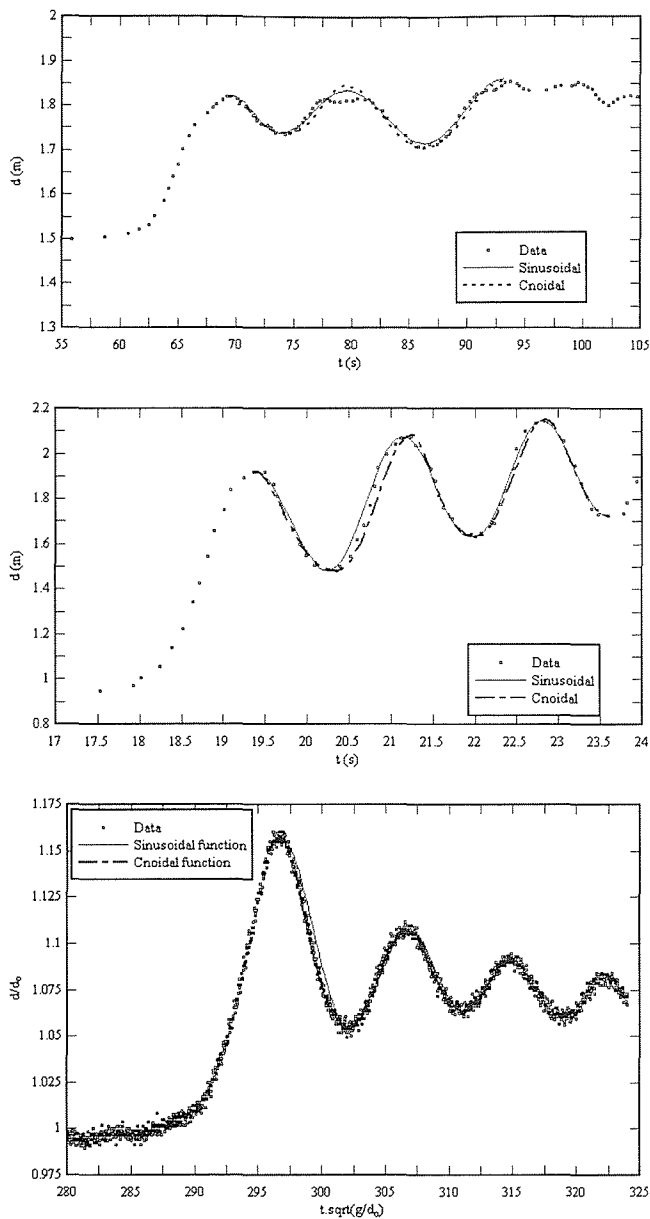


Fig. 4. Free-surface profile of an undular tidal bore: time variation in the flow depth; comparison with the linear wave theory (sinusoidal) and Boussinesq equation solution (cnoidal): (a) Daly River tidal bore on 2 July 2003 at 07:30 (data: Wolanski et al. 2004), Site C, $d_o=1.5\text{--}4$ m, and $U=4.7$ m/s; (b) Dee River tidal bore on September 22, 1972 at 10:34 (data: Lewis 1972), Run 12, $d_o=0.941$ m, $F=1.5$, and $U=3.44$ m/s; and (c) laboratory data (present study): $Q=0.0299$ m³/s and $d_o=0.2055$ m at $x=5$ m, $F=1.10$, and $U=1.269$ m/s

locity (Donnelly and Chanson 2005), but it was not mentioned in the tidal bore literature.

For the undular tidal bore, the maximum wave amplitude a_w/d_o and steepness a_w/L_w were limited by the apparition of wave breaking at the first wave crest. The dimensionless data are presented in Fig. 5 corresponding to the first wavelength. All data sets are compared to the analytical solutions of Lemoine (1948) and Andersen (1978), respectively, based on the linear wave theory and the Boussinesq equations. For a bore Froude number slightly larger than unity, both the wave amplitude and wave steepness increased with an increasing bore Froude number F .

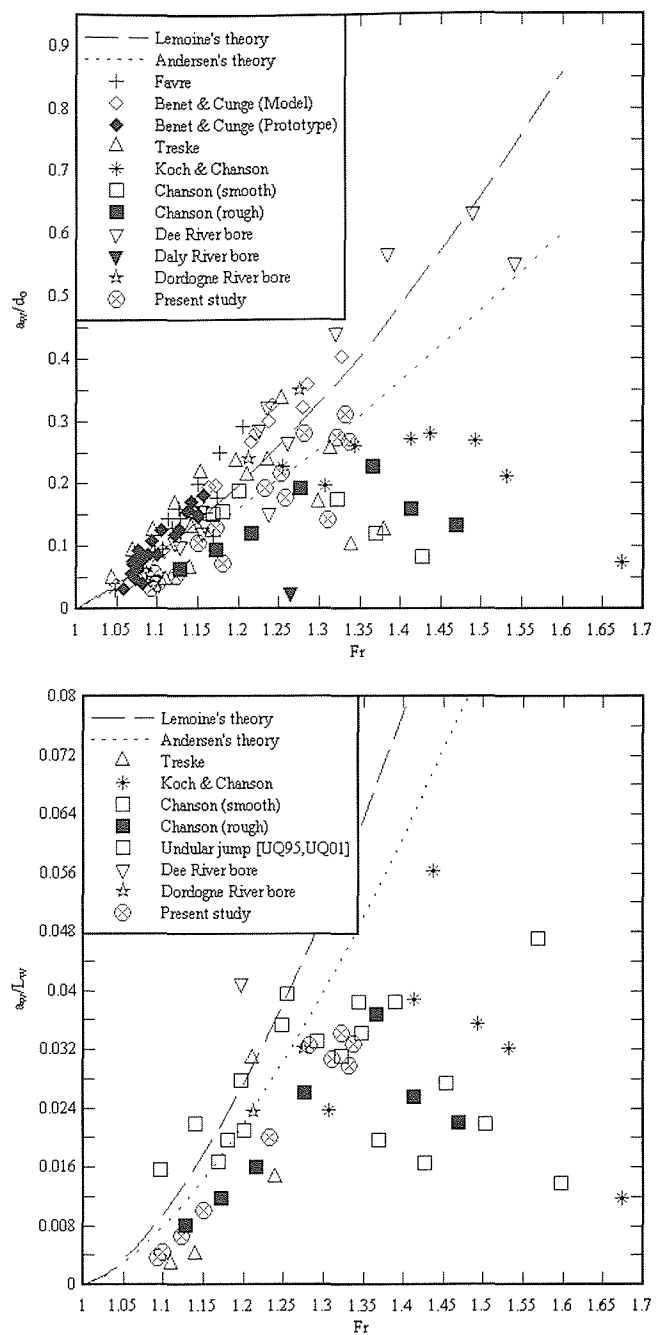


Fig. 5. Dimensionless wave properties in undular bore; data: present study, Favre (1935), Benet and Cunge (1971), Treske (1994), Koch and Chanson (2008), Chanson (2010), Lewis (1972) (Dee River tidal bore), Navarre (1995) (Dordogne River), and Wolanski et al. (2004) (Daly River tidal bore): (a) wave amplitude a_w/d_o ; (b) wave steepness a_w/L_w ; comparison with stationary undular hydraulic jump data: Montes and Chanson (1998) and Chanson (2005) (UQ95,UQ01)

However, both wave amplitude and steepness exhibited a maximum followed by a sharp decrease immediately before the disappearance of free-surface undulations. It is believed that the flow conditions associated with the maximum wave amplitude and wave steepness took place shortly before the appearance of small wave breaking at the first wave crest for $F\sim 1.3\text{--}1.4$. Note, in Fig. 5(b), that the undular bore data are compared also with some stationary hydraulic jump data. The data in Fig. 5 tended to follow more closely Lemoine's solution based on the linear wave

theory. While the Boussinesq equation is more accurate when the pressure distribution deviates from hydrostatic (i.e., $F=1.2-1.4$), the linear wave theory is simpler in practice, and the present results suggested that the linear wave theory yielded better results than the Boussinesq equation, justifying its usage in engineering practice. Importantly, the experimental data showed that both theories may be applicable only for a narrow range of Froude numbers. That is, for $1 \leq F < 1.3-1.35$ (Fig. 5).

Conclusions

A tidal bore is undular when its Froude number defined in the system of coordinates in translation with the bore is less than 1.5–1.8 corresponding to a ratio of conjugate depths less than 1.7–2.1. This study details the characteristics of undular bores including field observations (Table 1). The experimental results matched the $M-E$ function proposed by Benjamin and Lighthill (1954), implying that the rate of energy dissipation was small to negligible. The data analysis showed, however, that the approximation of hydrostatic pressure was inaccurate. The free-surface profile of the undulations presented a pattern somehow comparable to the sinusoidal and cnoidal wave functions, but neither captured the fine details of the undulation shape nor the asymmetrical wave profile. For small Froude numbers close to unity ($F < 1.3-1.35$), the wave amplitude and steepness results matched more closely the linear wave theory. The maximum wave amplitude and steepness data highlighted some maxima for $F=1.3-1.4$ corresponding to the apparition of some breaking at the first wave crest. Interestingly similar trends were observed for both field and laboratory data.

References

- Andersen, V. M. (1978). "Undular hydraulic jump." *J. Hydr. Div.*, 104(HY8), 1185–1188; "Discussion." 105(HY9), 1208–1211.
- Benet, F., and Cunge, J. A. (1971). "Analysis of experiments on secondary undulations caused by surge waves in trapezoidal channels." *J. Hydraul. Res.*, 9(1), 11–33.
- Benjamin, T. B., and Lighthill, M. J. (1954). "On cnoidal waves and bores." *Proc. R. Soc. London, Ser. A*, 224(1159), 448–460.
- Chanson, H. (1999). *The hydraulics of open channel flows: An introduction*, Edward Arnold, London.
- Chanson, H. (2005). "Physical modelling of the flow field in an undular tidal bore." *J. Hydraul. Res.*, 43(3), 234–244.
- Chanson, H. (2009). "An experimental study of tidal bore propagation: The impact of bridge piers and channel constriction." *Hydraulic Model Report No. CH74/09*, School of Civil Engineering, The Univ. of Queensland, Brisbane, Australia.
- Chanson, H. (2010). "Unsteady turbulence in tidal bores: The effects of bed roughness." *J. Waterway, Port, Coastal, Ocean Eng.*, 136(5), 247–256.
- Chanson, H., and Montes, J. S. (1995). "Characteristics of undular hydraulic jumps. Experimental apparatus and flow patterns." *J. Hydraul. Eng.*, 121(2), 129–144.
- Donnelly, C., and Chanson, H. (2005). "Environmental impact of undular tidal bores in tropical rivers." *Environ. Fluid Mech.*, 5(5), 481–494.
- Favre, H. (1935). *Etude théorique et expérimentale des ondes de translation dans les canaux découverts (Theoretical and experimental study of travelling surges in open channels)*, Dunod, Paris (in French).
- Henderson, F. M. (1966). *Open channel flow*, MacMillan Company, New York.
- Koch, C., and Chanson, H. (2008). "Turbulent mixing beneath an undular bore front." *J. Coastal Res.*, 24(4), 999–1007.
- Koch, C., and Chanson, H. (2009). "Turbulence measurements in positive surges and bores." *J. Hydraul. Res.*, 47(1), 29–40.
- Lemoine, R. (1948). *Sur les ondes positives de translation dans les canaux et sur le ressaut ondulé de faible amplitude (On the positive surges in channels and on the undular jumps of low wave height)*, La Houille Blanche, France, 183–185 (in French).
- Lewis, A. W. (1972). "Field studies of a tidal bore in the River Dee." M.S. thesis, Marine Science Laboratories, Univ. College of North Wales, Bangor, U.K.
- Liggett, J. A. (1994). *Fluid mechanics*, McGraw-Hill, New York.
- Montes, J. S. (1986). "A study of the undular jump profile." *Proc., 9th Australasian Fluid Mechanics Conf. (AFMC)*, Univ. of Auckland, Auckland, New Zealand, 148–151.
- Montes, J. S., and Chanson, H. (1998). "Characteristics of undular hydraulic jumps. Results and calculations." *J. Hydraul. Eng.*, 124(2), 192–205.
- Navarre, P. (1995). "Aspects physiques du caractères ondulatoire du Macaret en Dordogne (Physical features of the undulations of the Dordogne River tidal bore)." D.E.A. thesis, Univ. of Bordeaux, France (in French).
- Peregrine, D. H. (1966). "Calculations of the development of an undular bore." *J. Fluid Mech.*, 25, 321–330.
- Treske, A. (1994a). "Undular bores (Favre-waves) in open channels—Experimental studies." *J. Hydraul. Res.*, 32(3), 355–370; "Discussion." 33(3), 274–278.
- Wolanski, E., Williams, D., Spagnol, S., and Chanson, H. (2004). "Undular tidal bore dynamics in the Daly Estuary, Northern Australia." *Estuarine Coastal Shelf Sci.*, 60(4), 629–636.